Journal of Organometallic Chemistry, 427 (1992) 309–323
Elsevier Sequoia S.A., Lausanne
JOM 22450

The structure of $(^{i}Bu_3Sn)_2CO_3$ and $(Me_3Sn)_2CO_3$ in solution and in the solid state studied by $^{13}C/^{119}Sn$ NMR spectroscopy and X-ray diffraction

Jörg Kümmerlen, Angelika Sebald
Bayerisches Geo-Institut, Universität Bayreuth, Postfach 101251, W-8580 Bayreuth (Germany)

and Hans Reuter
Institut für Anorganische Chemie, Universität Bonn, Gerhard-Domagk-Str. 1, W-5300 Bonn (Germany)

(Received September 2, 1991)

Abstract

The structures of two bis(triorganotin) carbonates $(R_3Sn)_2CO_3$, with R = Me (**1a**) or ^{i}Bu (**1b**), have been determined by low temperature single crystal X-ray diffraction studies. The crystal structure of **1a** (previously determined at room temperature) has been redetermined at 200 K, at which the structure of **1b** has also been determined. Both compounds have similar polymeric structures; trigonal-planar R_3Sn moieties are axially bridged by bidentate $R_3Sn–O–CO_2$ units to trigonal-pyramidal R_3Sn moieties in such a way that helices parallel to the crystallographic *c*-axes are formed. There are differences in the number of the structural units $(R_3Sn^{tpy})(R_3Sn^{tpl})CO_3$ needed for a complete screw thread, namely, two for **1a** and four for **1b**. ^{13}C and ^{119}Sn high resolution solid-state NMR spectroscopy are consistent with the structural findings but also the existence of dynamic processes (on the NMR time scale) for solid **1a** at room temperature. Structural differences between the solid state and solution can be rationalised by comparison of solid and solution state NMR spectroscopy.

Introduction

Although bis(triorganotin)carbonates (**1**) have been known for more than a century [1] and have been investigated extensively during the past three decades, some doubts about their structures both in solution and in the solid state still remain. The first structural study was carried out by Sato and Okawara [2], who examined the IR spectrum of solid $(Me_3Sn)_2CO_3$ (**1a**). They proposed the monomeric structure **1** (see Scheme 1) for this compound, with each tin atom four

Correspondence to: Dr. A. Sebald, Bayerisches Geo-Institut, Universität Bayreuth, Postfach 101251, W-8580 Bayreuth, Germany.

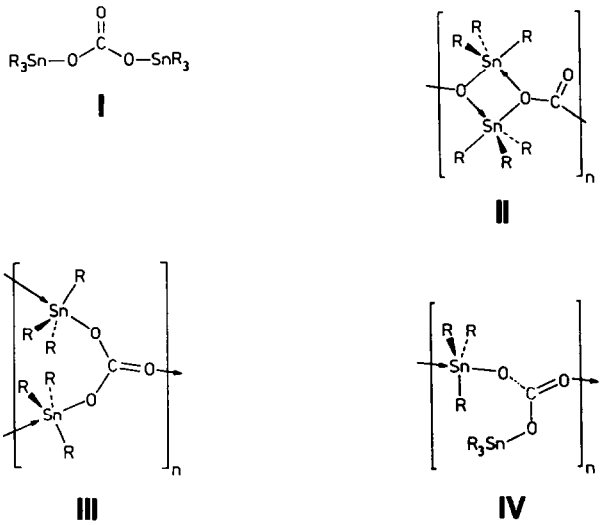

Scheme 1.

coordinate. This proposal was later adopted by Lohmann [3] who investigated the ethyl analogue.

On the basis of the Mössbauer spectrum of $(Cy_3Sn)_2CO_3$, Ho and Zuckermann [4] proposed the polymeric structure **II**, with trigonal-bipyramidal five-coordinate tin atoms bridged by bidentate carbonato groups. The quadrupole splitting data for this and for other bis(triorganotin) carbonates were found to be in better agreement with a *trans* than a *cis* configuration at pentacoordinate tin. In the light of this, Smith and Davies [5] suspected that the bis(triorganotin) carbonates have structure **III** in the solid state. In such a structure the carbonato groups would have to be tridentate, not bidentate.

Later better resolved Mössbauer data of **1** (R = Me, ^{n}Bu) showed the presence of two overlapping doublets, which can only be accounted for by assuming two non-equivalent R_3Sn moieties. On the basis of the observed values of the chemical shifts and quadrupole splittings for these doublets (which are in the range expected for trans trigonal-bipyramidal R_3SnX_2 and tetrahedral R_3SnX configurations, respectively), Blunden *et al.* [6] proposed the polymeric structure **IV**, with tridentate carbonato groups linking trigonal-planar and trigonal-pyramidal R_3Sn moieties. This structure was later confirmed for **1a** by a single crystal X-ray diffraction at room temperature [7]. Meanwhile Lockhart and Manders [8], finding only one broad resonance for the methyl carbons in the ^{13}C-CP-MAS NMR spectrum of this compound, had suggested a structure similar to structure **III**.

Blunden *et al.* [6] found that the ^{119}Sn NMR spectrum of $(^nBu_3Sn)_2CO_3$ in solution showed two broad resonances of nearly the same intensity, indicating that the tributyltin groups undergo exchange between four and five coordination at a rate commensurate with the NMR time scale. However, Lockhart found the ^{119}Sn NMR spectrum of $(Neophyl_3Sn)_2CO_3$ [9] in solution to contain only one signal with well resolved $^4J(^{119}Sn-^{117}Sn)$ coupling, consistent with the monomeric species I.

We present below a full description of the structures of bis(trimethyltin) (**1a**) and bis(tri-isobutyltin) carbonate (**1b**) in the solid state and in solution. We consider ^{13}C and ^{119}Sn solution and high resolution solid-state cross-polarisation magic-angle spinning NMR techniques, the results of low temperature single crystal X-ray diffraction studies, and some variable temperature CP MAS NMR data for the methyl compound (**1a**).

Experimental section

General procedures

Solvents (Aldrich) were of reagent grade and used without further purification. Microanalyses were carried out by the F. Pascher und E. Pascher, Microanalytical Laboratories, Remagen, Germany. Melting points were recorded on a Reichert melting point microscope and are uncorrected. ^{1}H, ^{13}C and ^{119}Sn solution state NMR spectra ($CDCl_3$) were recorded on a Bruker WH 90 NMR spectrometer operating at 90 MHz (^{1}H), 22.628 (^{13}C), and 33.546 (^{119}Sn) MHz, respectively. Chemical shifts for ^{1}H and ^{13}C were referenced to external tetramethylsilane (TMS), and those for ^{119}Sn to external tetramethyltin. The positive shift/high frequency (low field) convention is used throughout.

^{13}C and ^{119}Sn CP MAS NMR spectra were obtained on a Bruker MSL 300 NMR spectrometer, operating at 111.9 MHz for ^{119}Sn and at 75.2 MHz for ^{13}C, respectively. Standard double-bearing probes and 7 mm ZrO_2 rotors were used. The procedure for finding the $^{119}Sn-^{1}H$ matching condition has been described elsewhere [10]. Once again, ^{13}C and ^{119}Sn chemical shifts are relative to external TMS and tetramethyltin but were determined by use of solid adamantane (38.5 ppm) or tetracyclohexyltin (−97.35 ppm) as secondary external reference. The proton 90° pulse length was set at 5 μs, cross polarisation contact times were 1 ms (^{119}Sn) and 2 ms (^{13}C). Relaxation delays of 5 s were found to be satisfactory. Between 128 and 5600 transients were accumulated for ^{13}C (the cross polarisation efficiency being greatly enhanced at lower temperatures) and between 280 and 1100 transients for ^{119}Sn. The ^{119}Sn CP MAS NMR spectra were re-run at another, sufficiently different, spinning rate to allow unambiguous assignment of the centre band(s). Spinning rates were between 2.2 and 4.5 kHz. Variable temperature CP MAS NMR spectra were obtained for the temperature range 160–383 K with dry N_2 as drive and bearing gas.

Syntheses

Synthesis of $(Me_3Sn)_2CO_3$ (1a). A stream of dry carbon dioxide was passed for several hours through a solution of 1.81 g (10.0 mmol) of trimethyltin hydroxide in 250 ml of dry toluene. During the subsequent slow evaporation of the solvent at room temperature, **1a** separated as large transparent, colourless, crystals. Yield 1.36 g (70%); m.p. 200°C (lit. [11] 210°C). Anal. $C_7H_{19}O_3Sn_2$ calc.: C 21.86 (21.64), H 4.75 (4.93), Sn 60.5 (61.05)%. Trimethyltin hydroxide was prepared by a published procedure [12–14], starting from commercially available trimethyltin chloride (Merck–Schuchart).

Synthesis of $(^{i}Bu_3Sn)_2CO_3$ (1b). Dry carbon dioxide was bubbled for several hours through a solution of 3.0 g (5.0 mmol) of hexa-isobutyldistannoxane in 200 ml of dry acetone. During this time, transparent colourless crystals of **1b** formed on

Table 1

Experimental data for the X-ray diffraction study of $(Me_3Sn)_2CO_3$ and $(^iBu_3Sn)_2CO_3$

Compound	$(Me_3Sn)_2CO_3$	$(^iBu_3Sn)_2CO_3$
Crystal data		
Formula	$C_7H_{18}O_3Sn_2$	$C_{25}H_{54}O_3Sn_2$
Formula weight (g/mol)	387.60	640.08
Crystal system	Orthorhombic	Orthorhombic
Space group	$P2_12_12_1$	$P2_12_12_1$
Lattice constants		
a (pm)	704.6(2)	2116.7(8)
b (pm)	1870.5(2)	1471.8(7)
c (pm)	1012.2(2)	2048.3(6)
Cell volume (nm^3)	1.334	6.381
Formula units	4	8
Calc. density (g/cm^3)	1.930	1.333
μ (Mo-K_α) (cm^{-1})	34.50	14.56
Data collection		
Reflections collected/$2\theta_{max}$ (°)	3899/60.0	3844/42.0
Reflections observed	3792	3600
Unique reflections/R_{int}	3450/0.031	3600/0.0
Reflections suppressed with $F_o \leqq 2[\sigma(F_o)]$	51	342
Structure refinement		
Reflections used	3399	3258
Parameter refined	79	261
Data/parameter	43.03	12.48
R-value	0.043	0.061
R_w-value	0.050	0.068

the surface of the flask; these crystals had a rod-shaped habit but were seemingly twinned. After removal of the solvent, single crystals formed slowly from the residual viscous oil. Yield 2.21 g (68%); m.p. 75–86°C; Anal. $C_{25}H_{54}O_3Sn_2$ calc.: C 46.88 (46.91), H 8.50 (8.50), Sn 36.5 (37.09)%. Hexa-iso-butyldistannoxane was

Table 2

Fractional coordinates and isotropic displacement factors ($\times 10^{-2}$ nm^2) for $(Me_3Sn)_2CO_3$

	x	y	z	U
Sn(1)	0.31309(6)	−0.03209(2)	0.44282(3)	0.036(1) [a]
C(110)	0.0095(10)	−0.0284(3)	0.4566(6)	0.046(1)
C(120)	0.4917(11)	0.0459(4)	0.5309(7)	0.052(1)
C(130)	0.4342(13)	−0.1166(4)	0.3292(9)	0.062(2)
Sn(2)	−0.04391(6)	0.19924(2)	0.29934(3)	0.038(1) [a]
C(210)	0.0973(12)	0.2792(4)	0.1863(9)	0.060(2)
C(220)	−0.2864(15)	0.1545(5)	0.2059(10)	0.072(2)
C(230)	−0.0937(12)	0.2246(4)	0.5019(8)	0.056(2)
O(1)	0.3004(7)	0.0275(2)	0.2502(4)	0.045(2) [a]
O(2)	0.1512(7)	0.1217(2)	0.3347(4)	0.042(2) [a]
O(3)	0.1534(9)	0.1058(3)	0.1180(4)	0.050(2) [a]
C(1)	0.2027(10)	0.0835(3)	0.2335(5)	0.040(3) [a]

[a] Equivalent isotropic displacement factor $U_{eq} = 1/3\Sigma_i\Sigma_j U_{ij} a_i^* a_j^* (\boldsymbol{a}_i \cdot \boldsymbol{a}_j)$.

Table 3

Fractional coordinates and isotropic displacement factors ($\times 10^2$ nm^2) for $(^i Bu_3Sn)_2CO_3$

	x	y	z	U
Sn(1)	0.64950(6)	0.47643(9)	0.51257(6)	0.050(1) [a]
C(110)	0.6064(10)	0.3754(15)	0.5761(11)	0.068(6)
C(111)	0.5721(15)	0.4046(23)	0.6395(16)	0.114(10)
C(112)	0.5181(19)	0.4633(28)	0.6229(19)	0.144(13)
C(113)	0.5487(17)	0.3211(25)	0.6752(17)	0.132(12)
C(120)	0.6020(10)	0.5699(16)	0.4549(11)	0.071(6)
C(121)	0.5489(17)	0.5408(25)	0.4089(16)	0.123(10)
C(122)	0.5008(18)	0.4838(27)	0.4344(19)	0.139(13)
C(123)	0.5224(24)	0.6285(36)	0.3760(22)	0.190(19)
C(130)	0.7501(10)	0.4569(15)	0.5169(10)	0.066(5)
C(131)	0.7915(11)	0.5475(17)	0.5141(11)	0.075(6)
C(132)	0.7831(11)	0.5996(17)	0.4531(13)	0.076(6)
C(133)	0.8601(13)	0.5204(18)	0.5269(13)	0.090(7)
Sn(2)	0.64466(7)	0.78703(11)	0.62355(7)	0.062(1) [a]
C(210)	0.5464(12)	0.7483(18)	0.6293(12)	0.086(7)
C(211)	0.5034(27)	0.7623(43)	0.5665(28)	0.216(24)
C(212)	0.5047(22)	0.8473(35)	0.5431(21)	0.163(16)
C(213)	0.4362(27)	0.7450(43)	0.6127(28)	0.224(23)
C(220)	0.6864(11)	0.8072(15)	0.5307(11)	0.070(6)
C(221)	0.7473(12)	0.8539(18)	0.5327(13)	0.085(7)
C(222)	0.7714(17)	0.8754(26)	0.4611(18)	0.126(11)
C(223)	0.7959(14)	0.8247(20)	0.5719(14)	0.098(8)
C(230)	0.6682(10)	0.8820(16)	0.6992(11)	0.073(6)
C(231)	0.6244(11)	0.9642(17)	0.7073(11)	0.079(7)
C(232)	0.6392(16)	1.0202(22)	0.7643(17)	0.119(10)
C(233)	0.6275(16)	1.0144(23)	0.6389(16)	0.117(10)
O(1)	0.6521(6)	0.5924(9)	0.5847(6)	0.058(3)
C(1)	0.6844(8)	0.5960(12)	0.6386(9)	0.044(4)
O(2)	0.6913(6)	0.6773(8)	0.6637(6)	0.052(3)
O(3)	0.7080(5)	0.5309(8)	0.6670(5)	0.043(3)
Sn(3)	0.75956(5)	0.54977(8)	0.76224(6)	0.043(1) [a]
C(310)	0.8309(8)	0.6255(12)	0.7126(9)	0.048(5)
C(311)	0.8991(10)	0.6137(15)	0.7350(11)	0.071(6)
C(312)	0.9281(12)	0.5255(18)	0.7207(13)	0.090(8)
C(313)	0.9361(17)	0.6907(24)	0.7003(17)	0.124(11)
C(320)	0.7683(9)	0.4016(14)	0.7786(11)	0.060(5)
C(321)	0.7529(13)	0.3384(20)	0.7220(14)	0.101(8)
C(322)	0.7447(17)	0.2429(28)	0.7502(17)	0.148(14)
C(323)	0.8118(21)	0.3410(30)	0.6822(21)	0.161(15)
C(330)	0.6812(8)	0.6161(12)	0.8060(9)	0.049(5)
C(331)	0.6128(9)	0.5877(14)	0.7859(10)	0.060(5)
C(332)	0.5988(13)	0.4921(18)	0.8094(13)	0.089(8)
C(333)	0.5673(14)	0.6576(19)	0.8174(14)	0.099(8)
Sn(4)	0.85250(7)	0.82589(10)	0.88595(7)	0.062(1) [a]
C(410)	0.9511(13)	0.8016(18)	0.8935(13)	0.086(7)
C(411)	0.9780(15)	0.8150(19)	0.9625(14)	0.098(9)
C(412)	1.0482(17)	0.7876(26)	0.9622(17)	0.130(11)
C(413)	0.9770(16)	0.9186(23)	0.9794(16)	0.119(10)
C(420)	0.8035(11)	0.8581(16)	0.9753(11)	0.071(6)
C(421)	0.7393(18)	0.8315(26)	0.9779(18)	0.134(12)
C(422)	0.6938(13)	0.8417(19)	0.9238(14)	0.092(8)
C(423)	0.7066(16)	0.8679(25)	1.0448(17)	0.122(11)
C(430)	0.8280(11)	0.9042(17)	0.7992(12)	0.082(7)

Table 3 (continued)

	x	y	z	U
C(431)	0.8766(13)	0.9743(19)	0.7803(14)	0.096(8)
C(432)	0.8594(15)	1.0215(20)	0.7157(15)	0.107(9)
C(433)	0.8768(17)	1.0512(25)	0.8355(17)	0.129(11)
O(4)	0.8087(6)	0.5577(9)	0.8607(6)	0.055(3)
C(2)	0.8258(9)	0.6369(13)	0.8827(9)	0.053(5)
O(5)	0.8152(6)	0.7088(8)	0.8524(6)	0.053(3)
O(6)	0.8545(6)	0.6391(9)	0.9400(6)	0.054(3)

[a] Equivalent isotropic displacement factor $U_{eq} = 1/3\Sigma_i\Sigma_j U_{ij} a_i^* a_j^* (\boldsymbol{a}_i \cdot \boldsymbol{a}_j)$.

Table 4

Selected bond lengths (pm) and angles (°) for $(Me_3Sn)_2CO_3$ and $(^iBu_3Sn)_2CO_3$

$(Me_3Sn)_2CO_3$		$(^iBu_3Sn)_2CO_3$		
Bond lengths (pm)				
Sn(1)–O(2)	224.8(4)	225.8(13)	Sn(3)–O(3)	225.3(11)
Sn(1)–O(3′)	225.8(4)	226.1(12) [a]	Sn(3)–O(4)	227.2(13)
Sn(1)–C(110)	214.5(7)	217.7(22)	Sn(3)–C(310)	213.4(18)
Sn(1)–C(120)	212.3(7)	207.4(23)	Sn(3)–C(320)	221.4(21)
Sn(1)–C(130)	213.3(9)	215.1(21)	Sn(3)–C(330)	212.3(18)
Sn(2)–O(2)	203.1(5)	206.3(12)	Sn(4)–O(5)	201.4(12)
Sn(2)–C(210)	212.9(9)	216.0(26)	Sn(4)–C(410)	212.4(27)
Sn(2)–C(220)	212.5(11)	211.8(23)	Sn(4)–C(420)	215.6(23)
Sn(2)–C(230)	213.4(8)	214.6(23)	Sn(4)–C(430)	218.1(25)
C(1)–O(1)	126.3(7)	130.0(22)	C(2)–O(4)	130.0(23)
C(1)–O(2)	130.1(7)	131.1(22)	C(2)–O(5)	124.7(23)
C(1)–O(3)	128.9(7)	122.7(21)	C(2)–O(6)	132.1(22)
O(1)–Sn(1)	224.8(4)	225.8(13)	O(4)–Sn(3)	227.2(13)
O(2)–Sn(2)	203.1(5)	206.3(12)	O(5)–Sn(4)	201.7(12)
O(3)–Sn(1′)	225.8(4)	225.3(11) [a]	O(6)–Sn(1′)	226.1(12)
Bond angles (°)				
O(1)–Sn(1)–O(3′)	171.1(2)	179.2(7)	O(3)–Sn(3)–O(4)	175.5(5)
O(1)–Sn(1)–C(110)	90.0(2)	97.8(7)	O(3)–Sn(3)–C(310)	89.6(5)
O(1)–Sn(1)–C(120)	92.7(2)	83.3(7)	O(3)–Sn(3)–C(320)	92.9(6)
O(1)–Sn(1)–C(130)	85.2(3)	92.9(7)	O(3)–Sn(3)–C(330)	92.5(6)
O(3′)–Sn(1)–C(110)	94.2(2)	82.2(7) [a]	O(4)–Sn(3)–C(310)	94.1(6)
O(3′)–Sn(1)–C(120)	91.6(2)	96.1(7) [a]	O(4)–Sn(3)–C(320)	83.0(6)
O(3′)–Sn(1)–C(130)	85.9(2)	87.9(6) [a]	O(4)–Sn(3)–C(330)	87.7(6)
C(110)–Sn(1)–C(120)	122.8(3)	126.2(8)	C(310)–Sn(3)–C(320)	121.8(7)
C(120)–Sn(1)–C(130)	119.9(3)	126.3(8)	C(320)–Sn(3)–C(330)	120.9(7)
C(130)–Sn(1)–C(110)	117.3(3)	107.4(8)	C(330)–Sn(3)–C(310)	117.0(7)
O(2)–Sn(2)–C(210)	106.2(3)	103.4(8)	O(5)–Sn(4)–C(410)	105.4(8)
O(2)–Sn(2)–C(220)	110.0(3)	105.5(7)	O(5)–Sn(4)–C(420)	106.8(7)
O(2)–Sn(2)–C(230)	95.8(2)	96.4(7)	O(5)–Sn(4)–C(430)	94.6(8)
C(210)–Sn(2)–C(220)	114.4(4)	119.2(9)	C(410)–Sn(4)–C(420)	116.6(9)
C(220)–Sn(2)–C(230)	122.5(4)	117.4(9)	C(420)–Sn(4)–C(430)	112.5(10)
C(230)–Sn(2)–C(210)	115.9(3)	110.9(9)	C(430)–Sn(4)–C(410)	117.4(9)
O(1)–C(1)–O92)	120.1(5)	115.4(15)	O(4)–C(2)–O(5)	122.5(17)
O(2)–C(1)–O(3)	117.4(5)	118.8(15)	O(5)–C(2)–O(6)	120.2(17)
O(3)–C(1)–O(1)	122.4(5)	125.8(16)	O(6)–C(2)–O(4)	117.3(16)
C(1)–O(1)–Sn(1)	123.3(3)	126.8(11)	C(4)–O(4)–Sn(3)	118.8(11)
C(1)–O(2)–Sn(2)	116.3(3)	120.4(11)	C(4)–O(5)–Sn(4)	119.0(12)
C(1)–O(3)–Sn(1′)	119.1(4)	120.8(11)	C(4)–O(5)–Sn(1′)	123.2(11)

[a] For $(^iBu_3Sn)_2C_3$ atom O(3′) is to be replaced by O(6′) and Sn(1′) by Sn(3); compare Fig. 1.

prepared by hydrolysis of tri-isobutyltin chloride [15,16]. Yield 4.11 g (69%); b.p. 141–143°C/0.1 Torr (lit. [17] 142–146°C/0.001 Torr). ^{13}C NMR: δ(C-1) 28.8 ($^{1}J(^{13}C-^{119}Sn) = 364.0$ Hz) δ(C-2) 26.5 ($^{2}J(^{13}C-^{119}Sn) = 17.6$ Hz) δ(C − 3) 26.9 ($^{3}J(^{13}C-^{119}Sn) = 43.9$ Hz) ppm. ^{119}Sn NMR: δ(Sn) 77.7 ($^{2}J(^{119}Sn-^{117}Sn) = 443.1$ Hz) ppm. IR: ν_{as}(Sn–O) = 778 cm^{-1}.

X-Ray diffraction studies

Determination of lattice constants and collection of intensity data were performed on an Enraf–Nonius CAD4 automated diffractometer using Mo-K_α radiation and graphite monochromator at 200 K. Unit cell parameters were derived from a least-squares analysis of the setting angles of 25 reflections in the range $18.98° \leq 2\theta \leq 28.36°$ for **1a** and $22.70° \leq 2\theta \leq 35.10°$ for **1b**, respectively. Intensity data were collected in the octants $\pm h,k,l$ (**1a**) and h,k,l (**1b**) using a variable speed ω–2θ–scan mode and corrected for Lorentz and polarization effects. The intensities and orientations of two standard reflections were monitored every hour and every 200 reflections, respectively, and showed no significant variation.

The crystals were orthorhombic with systematic absences $h\ 0\ 0 = 2n$, $0\ k\ 0 = 2n$ and $0\ 0\ l = 2n$ strongly indicative of the non-centrosymmetric space group $P2_12_12_1$ (no. 19 [18]). The structures were solved by the direct methods using SHELXS-86 [19] followed by difference Fourier syntheses. Refinements were performed with full-matrix least-squares methods of SHELX-76 [20] using appropriate neutral scattering factors and anomalous scattering terms. The function minimized was $R_f = \Sigma w(|F_o| - |F_c|)^2$ with $w = 1/[\sigma^2(F_o) + 0.00498 \times F_o^2]$ for **1a** and $w = 1/[\sigma^2(F_o) + 0.00899 \times F_o^2]$ for **1b**. R values were calculated as $R_w = \Sigma\sqrt{w}\,||F_o| - |F_c||/\Sigma\sqrt{w}\,|F_o|$ and $R = \Sigma||F_o| - |F_c||/|F_o|$.

A final difference Fourier map did not reveal any features except for those associated with some of the hydrogen atoms from the organic groups. Experimental data for the X-ray diffraction study of both compounds are collected in Table 1. Plots were derived by KPLOT [21] and drawn by ORTEP [22]. Final fractional atomic coordinates and isotropic displacement factors are shown in Tables 2, 3. Selected distances and bond angles are listed in Table 4. Tables of anisotropic displacement factors along with a listing of observed structure factor amplitudes are available from the authors.

Results and discussion

Crystal structures

In the solid state both compounds **1a** and **1b** show the same structural feature with trigonal-planar (tpl) R_3Sn moieties axially bridged by bidentate R_3Sn–O–CO_2 units to trigonal-pyramidal (tpy) R_3Sn moieties in such a way that polymeric chains, winding around the twofold screw axes parallel to the crystallographic c axes, are formed.

This structural feature had previously been observed [7] for **1a** at room temperature but due to the differences between the room temperature and the low temperature ^{13}C CP MAS NMR spectra (see below) of this compound, it was necessary to check whether the structure changed at lower temperatures. Evidently, there is no major change detectable by X-ray diffraction.

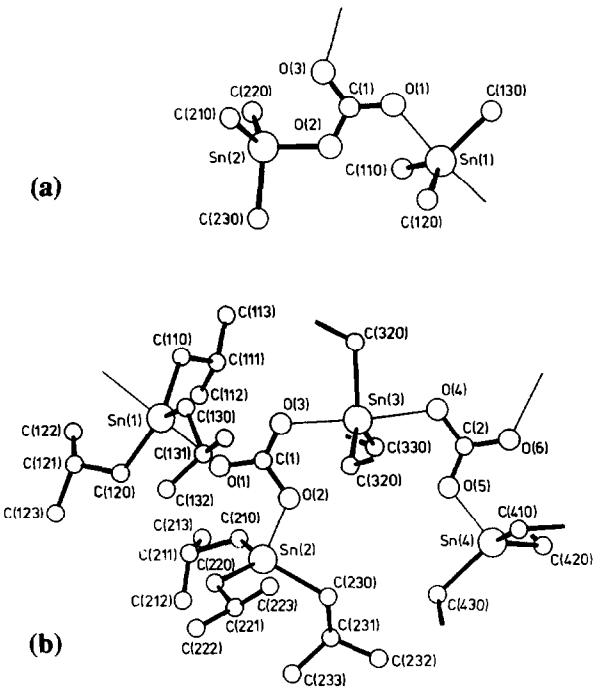

Fig. 1. Perspective view of the asymmetric units in the polymeric crystal structure of $(Me_3Sn)_2CO_3$ (a) and $(^iBu_3Sn)_2CO_3$ (b) showing the numbering scheme. Some carbon atoms of the isobutyl groups are omitted for clarity. Their numbering follows the scheme used for the carbon atoms shown for the other isobutyl groups.

Although **1a** and **1b** crystallize in the same space group ($P2_12_12_1$) and both are built up from the same structural units they are not isostructural. The main difference results from the fact that two structural units $(R_3Sn^{tpy})(R_3Sn^{tpl})CO_3$ are involved in building the asymmetric unit in **1b** whereas it is only one in the case of **1a** (Fig. 1). That means that four formula units complete a screw thread in **1b** but only two in **1a** (Fig. 2). The reason for this must lie in the different steric requirements of the two different organic groups: the smaller methyl group will allow a more compact arrangement of the chains than does the bigger isobutyl group. For the same reason **1a** has a much higher density (1.930 g/cm^3) than **1b** (1.333 g/cm^3).

Except for this minor structural variation there are no significant differences between the two structures. In both, the coordination sphere of the two different tin atoms (Sn^{tpy}, Sn^{tpl}) in the structural unit is completed by one or two oxygen atoms of the carbonato groups, resulting in a tetrahedral (th) and a trigonal-bipyramidal (tbp) environment, respectively for the atoms.

Within the coordination sphere of Sn^{tbp}, the observed tin–oxygen distances (224.8–227.2 pm, Table 3) are remarkably long compared with the normal Sn–O distance of 199.9 pm observed in Mes_3SnOH [23] or some unusually short ones (189.3–197.2 ppm) found in hexaorganodistannoxanes [24–28] $(R_3Sn)_2O$ and hexaorganocyclotristannoxanes [29–32] $(R_2SnO)_3$. This effect is due to the axial position that the oxygen atoms occupy in the trigonal bipyramid. Comparably long

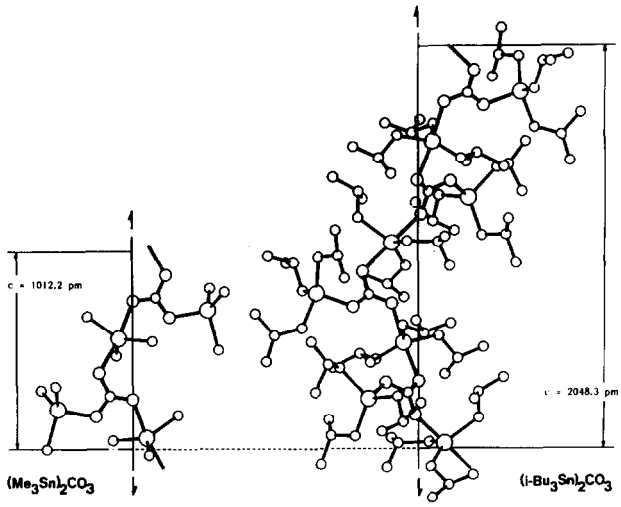

Fig. 2. Comparison of the crystal structures of **1a** and **1b**. In both cases the projection of a complete thread into the *ab*-plane and the directions of the crystallographic screw axes parallel to *c* are shown. Because of the different number of building units used the *c*-axis of **1b** is twice as long as the *c*-axis of **1a**.

Sn–O bond lengths are found in some other types of organotin compounds such as triorganotin hydroxides R_3SnOH [27,33–35] and 1-chloro-3-hydroxy-1,1,3,3-tetra-organodistannoxanes [27,36,37] $(R_2SnCl)(R_2SnOH)O$ in which the location of the hydroxyl group is very similar to that of the carbonato group in the coordination sphere of Sn^{tpl} in **1**.

The Sn–O distances in the coordination sphere of Sn^{tbp} are much longer than those in the environment of Sn^{th} (201.7–206.3 pm). The latter values differ only slightly from normal tin–oxygen bond lengths because the bonding situation is very similar; with the tin atom in a four-coordinate tetrahedral environment and the oxygen atom two-coordinate.

Results of NMR studies

The ^{119}Sn CP MAS NMR spectra of **1a** and **1b** are shown in Fig. 3. Figure 4 shows ^{13}C CP MAS NMR spectra of **1a** at various temperatures. Table 5 lists the ^{13}C and ^{119}Sn NMR data for **1a** and **1b**, Table 6 the tensorial components of the ^{119}Sn shielding for **1a**, **b**, and Table 7 the cross polarisation characteristics for **1a** at 200 and 283 K, which are also shown in Fig. 5.

In general, the ^{13}C and ^{119}Sn CP MAS NMR data for **1a** and **1b** are in very good agreement with the crystallographic results, but some further comment is appropriate. The ^{119}Sn CP MAS NMR spectra for **1a** and **1b** (see Fig. 3) are consistent with the structural features evident from the crystal structure: for both compounds ^{119}Sn resonances for four-coordinate tin (+123.3 and 85.5 ppm, respectively) and five-coordinate tin (−62.2 and −75.2, −96.4 ppm, respectively) are found at room temperature. The appearance of two ^{119}Sn resonances for solid **1a** are in agreement with the X-ray crystallographic results. The crystal structure would suggest the presence of four ^{119}Sn resonances for **1b**, whereas we observed only three in an approximately 2:1:1 intensity ratio (see Fig. 3). This is at-

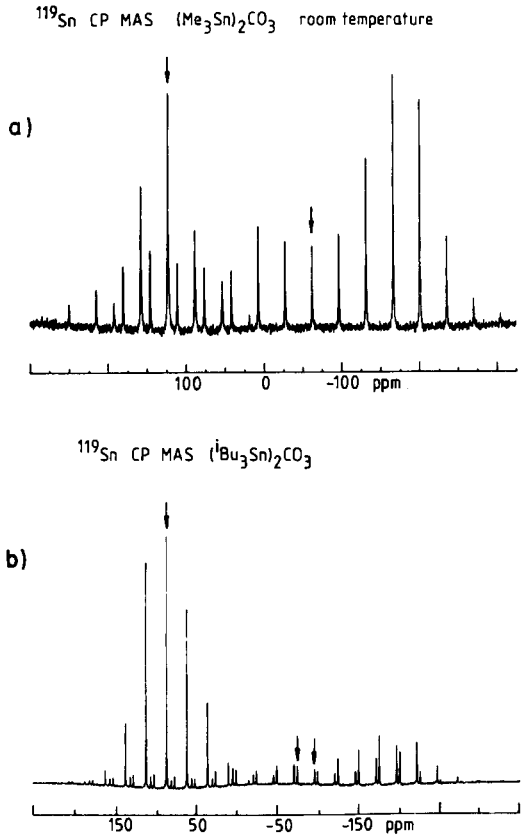

Fig. 3. ^{119}Sn CP MAS NMR spectra of **1a**, $(Me_3Sn)_2CO_3$ (a) and **1b**, $(^tBu_3Sn)_2CO_3$ (b), obtained at room temperature. Experimental conditions: (a) spinning rate 3.9 kHz, 2940 transients, 5 s recycle delay, 1 ms contact time; (b) spinning rate 2.8 kHz, 1180 transients, 5 s recycle delay, 1 ms contact time. No linebroadening was used prior to Fourier transformation.

tributable to the fact that the two tetrahedral tin atoms Sn(4) and Sn(2) in **1b** are crystallographically related by a pseudo-screw axis which renders these two positions chemically equivalent.

The chemical shifts $\delta(^{119}Sn)$ found for solid **1a** and **1b** can be regarded typical for organotin compounds involving the two types of coordination present in **1a** and **1b** [28,38–42]. It should also be mentioned that the shift differences between the tetrahedral and the five-coordinate tin atom in **1a** (185 ppm) and **1b** (approx. 170 ppm) fall into the usual range (approx. 150–250 ppm) for the increase in ^{119}Sn shielding on going from tetrahedral to five-coordination. In this respect the solution state ^{119}Sn chemical shift of 101.7 ppm for **1b** is only moderately different from that for the tetrahedral tin in solid **1b** (see Table 5). In view of the polymeric crystal structure, it is understandable that bis(trioganotin) carbonates are only sparingly soluble in most inert organic solvents. This solubility is lowest for the methyl compound, and increases somewhat when larger alkyl groups are introduced. Thus well-resolved ^{13}C and ^{119}Sn solution state NMR spectra were obtained only for **1b**, for which the number of resonances, their narrow line widths,

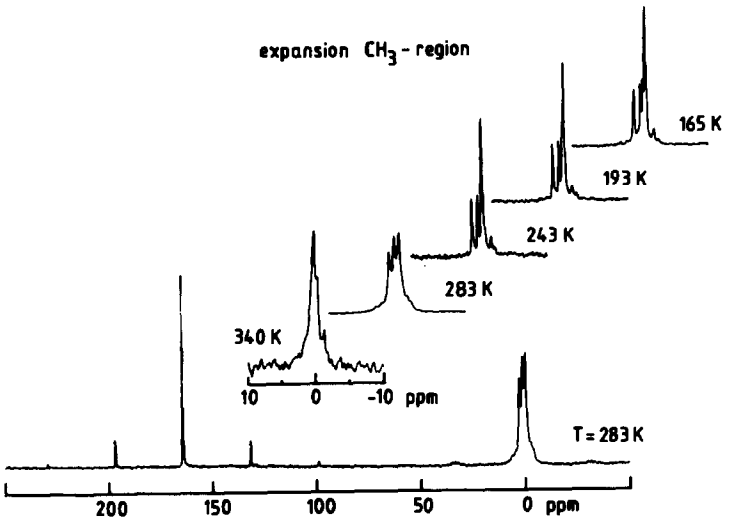

Fig. 4. ^{13}C CP MAS NMR spectrum of **1a**, $(Me_3Sn)_2CO_3$ at 283 K. The expansion shows the methyl region at various temperatures.

the different pairs of ^{119}Sn and ^{13}C satellites, indicate that the solution must contain monomeric molecules of structural type **I** (see Scheme 1). Moreover, there is no evidence that oligomers are formed in solution or that there is exchange between the monomeric molecules.

The solution state ^{13}C NMR spectrum of **1b** has to be assigned as follows: δ(C-1) 29.5 ($^1J(^{119}Sn^{13}C) = 356.0$ Hz); δ(C-2) = 26.2 ($^2J(^{13}C^{119}Sn) = 17.6$ Hz); δ(C-3) 26.7 ($^3J(^{13}C^{119}Sn) = 50.5$ Hz) ppm. The resonance of the $^{13}CO_3$ carbon is observed at 162.3 ppm. Evidently this value does not change on going from the

Table 5

^{13}C and ^{119}Sn NMR data of $(Me_3Sn)_2CO_3$ and $(^iBu_3Sn)_2CO_3$ at room temperature [a]

	$\delta(^{119}Sn)$ (ppm)		$\delta(^{13}C)$ (ppm) ($^nJ(^{119}Sn^{13}C)$)	
	Solution ($CDCl_3$)	Solid ($\nu_{1/2}$ in Hz)	Solution ($CDCl_3$)	Solid
1a $(Me_3Sn)_2CO_3$	[b]	+123.5 (150) −62.2 (120)	[b]	2.2 0.7 −0.7 ≈ −1; broad 163.8
1b $(^iBu_3Sn)_2CO_3$	+101.7	+86.5 (30) −75.1 (40) −96.4 (40)	29.5 (356.0) 26.2 (17.6) 26.7 (50.5) 162.2	33.9 27.3 [c] 32.9 26.9 32.3 26.1 29.2 28.7 163.3 27.9

[a] See experimental part for technical details. [b] Not soluble enough for ^{13}C and ^{119}Sn NMR in $CDCl_3$; ^1H NMR: $\delta(CH_3)+0.43$ ($^2J(^{119/117}Sn^1H) = 57$ Hz) ppm. [c] Aliphatic region displays an unresolved multiplet with maxima as indicated.

Table 6

^{119}Sn shielding tensor data for **1a**, **b** [a]

	δ_{iso} (ppm)	σ_{iso} (ppm)	σ_{11}	σ_{22} (ppm)	σ_{33}	δ_A (ppm)	$\Delta\sigma$ (ppm)	η
1a	+123.5	−123.5	−188.5	−138.0	−43.7	79.6	120.0	0.63
	−62.0	+62.0	246.4	192.0	−252.2	−314.3	−471.4	0.17
1b	+86.5	−86.5	−146.9	−85.4	−25.1	60.7	91.1	0.99
	−75.1	+75.1	225.6	185.1	−185.2	−260.4	−390.0	0.15
	−96.4	+96.4	240.8	240.3	−203.5	−299.9	−449.8	0.0

[a] $\sigma_i = 1/3\ (\sigma_{33} + \sigma_{22} + \sigma_{11})$; $|\sigma_{33} - \sigma_i| \geq |\sigma_{11} - \sigma_i| \geq \sigma_{22} - \sigma_i|$. $\Delta\sigma = \sigma_{33} - 1/2\ (\sigma_{11} + \sigma_{22})$; $\Delta\sigma = 3/2\ \delta_A$. $\delta_A = \sigma_{33} - \sigma_i$. $\eta = 2/3\ (\sigma_{22} - \sigma_{11})\ (\Delta\sigma)^{-1}$.

solid state (see above) to solution even though the carbonato group is no longer tridentate (structure type IV) but bidentate (structure type I).

The ^{119}Sn NMR spectrum (in $CDCl_3$) reveals only one resonance for the bis(tri-iso-butyl-tin) carbonate, at 101.7 ppm. This observation supports the argument that the solution contains monomeric molecules of structure type I, in which both tin sites are equivalent and tetrahedrally coordinated. The spectrum also shows two pairs of ^{13}C satellites which, in the light of the values of the coupling constants derived from the ^{13}C NMR spectrum must be assigned to ^1J and $^3J(^{119}Sn-^{13}C)$, respectively. In contrast to Lockhart's [9] results, no $^4J(^{119}Sn-^{117}Sn)$ coupling could be detected.

Inspection of the ^{119}Sn tensorial data in Table 6 reveals that all three ^{119}Sn resonances assigned to the five-coordinate tin in solid **1a**, **b**, display axially symmetric shielding tensors and shielding anisotropies $\Delta\sigma$ of the order of 400 ppm. This agrees well with the *trans*-geometry around these tin atoms: in the light of the data for, *e.g.*, solid Me_3SnOH[43] ($\eta = 0.57$ and $\Delta\sigma = 264$ ppm), a less pronounced transoid geometry might be expected for the Me_3SnO_2 moiety in solid Me_3SnOH, which has not been studied by X-ray diffraction. The tetrahedrally coordinated tin sites for **1a**, **b** show asymmetric shielding tensors ($\eta = 0.60$ and 0.99, respectively), in line with a strongly distorted tetrahedral environment. The difference between the η values, 63.0 and 0.99, is significant and must be attributed to the steric requirements of the bulky isobutyl ligands in **1b**. At first glance it may seem surprising that this tetrahedral R_3SnO moiety exhibits such a

Table 7

^{119}Sn cross polarisation characteristics for $(Me_3Sn)_2CO_3$, **1a** for two different temperatures [a]

	σ_{iso} (ppm)	I_0 (a.u.)	T_{IS} (ms)	$T_{1\rho}$ (ms)
$T = 283$ K	62.2	3.40	1.21	0.37
	−123.5	2.05	1.32	1.19
$T = 200$ K	65.5	5.64	0.63	27.51
	−125.3	4.49	0.72	42.73

[a] A detailed description of the procedure to fit CP curves by a bi-exponential equation is given in refs. 44 and 47.

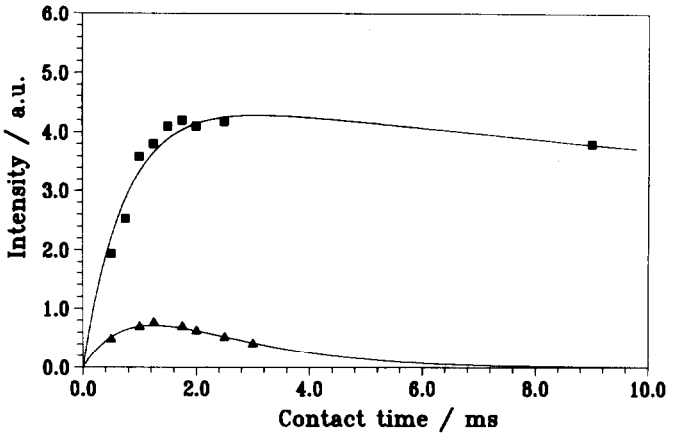

Fig. 5. Plot of the integrated intensity of the high-field (−62.2 ppm) ^{119}Sn resonance of solid **1a** at 200 K (■) and at 293 K (▲) *versus* the $^{1}H \rightarrow {}^{119}Sn$ contact time.

strongly asymmetric shielding tensor: the Sn–O bond might have been expected to introduce a "pseudo C_3 symmetry". Unfortunately, to date there are not enough ^{119}Sn shielding tensor data in the literature to enable us to put this observation in perspective. Future ^{119}Sn CP MAS NMR studies of organometallic tin compounds will help to overcome this problem.

The ^{13}C CP MAS spectra of **1a** at various temperatures (Fig. 4) shows that a dynamic process involving at least one of the two Me_3Sn groups must occur in this temperature range and at a rate commensurate with the NMR time-scale. As mentioned before, X-ray crystallography failed to identify this process but it is clear that no major structural changes occur. This conclusion was corroborated by variable temperature ^{119}Sn CP MAS spectroscopy: over the temperature range 160–293 K the isotropic ^{119}Sn chemical shifts for **1a** change very little, and as a linear function of temperature (Sn^{th} 0.05 ppm/K and Sn^{tbp} 0.02 ppm/K), and furthermore, the overall shape of the ^{119}Sn shielding tensor pattern remains unchanged. Similarly, the isotropic ^{13}C shifts do not change much as a function of temperature, and so in this again any phase transitions or major structural changes can be excluded.

The ^{13}C resonance for one of the two Me_3Sn groups appears to be in a coalescence region near room temperature and sharpens considerably as the temperature is lowered (see Fig. 4, at 193 K and below, the satellites due to the coupling $^{1}J(^{119/117}Sn^{13}C)$ of 380 Hz are readily seen).

Another indication of this dynamic process comes from the spin dynamics of the ^{119}Sn cross polarisation experiment itself. As depicted in Fig. 5 and Table 7, the CP efficiency for **1a** increases greatly as the temperature is lowered; at low temperature $T_{1\rho}$ is very long whereas T_{IS} becomes fairly short. Any motional process will scale the dipole–dipole interactions responsible for the efficiency of the polarisation transfer, thus making the CP experiment less efficient. At low temperatures, *i.e.* when the dynamic process is significantly slower, the full breadth of the dipole–dipole interaction becomes available, and T_{IS} is accordingly much shorter. Similarly, at low temperature equivalent to a more rigid lattice and longer correlation times τ_c, $T_{1\rho}$ will generally increase. The qualitative trends in the CP

dynamics of **1a** could in principle be attributed to a dynamic process such as internal rotation of the various methyl-groups, but at such fairly high temperatures it is most unlikely that such a dynamic process would be frozen [44,45]. Furthermore, if internal rotation of the methyl groups were solely responsible for this effect it would be impossible to explain why the two different Me_3Sn moieties in **1a** experience different time/CP efficiency regimes at a given temperature (see Table 7). Some other, fairly subtle, dynamic process must be responsible for this effect.

It seems reasonable to ascribe this dynamic process to the tetrahedral Me_3Sn moiety, with the assumption of a fairly rigid chain-building Me_3SnO_2/carbonate backbone. As judged from the variable temperature ^{119}Sn CP MAS data, the tetrahedral tin site itself cannot be involved directly, as this would have had visible effects on the ^{119}Sn CP MAS spectra. This leaves two possible mechanisms to account for the observed temperature effects, both requiring the Me_3Sn^{thl}–O bond as an axis of rotation, *i.e.* retained symmetry. One possibility would involve discrete movements around this axis, the other a small-scale diffusive motion of the three methyl groups around their equilibrium positions. As can be seen from the expanded inset in Fig. 4, at elevated temperatures the onset of motion for the (at room temperature fairly rigid) Me_3Sn^{tbp} groups becomes observable; the well-resolved 1:1:1 ^{13}C-triplet broadens considerably, leaving a fairly complex process to be explained.

Generally speaking, high resolution solid-state NMR spectroscopy does have the potential to distinguish between different mechanisms of motion, either by one-dimensional (lineshape analysis in the slow-motion regime) or by 2D-exchange methods. Such processes seem to be fairly common for solid trimethyltin compounds, and we have recently demonstrated that use of the full range of suitable solid-state NMR techniques can give unambiguous answers [46] with respect to the mechanisms involved. In the case of **1a**, however, the further application of NMR techniques is severely hampered; lineshape analysis is not informative since only one ^{13}C resonance is observed for the Me_3Sn^{thl} group, and meaningful 2D-exchange spectroscopy is precluded by the marked overlap of this resonance with those of the Me_3Sn^{tbp} moiety.

The ^{13}C CP MAS NMR spectrum of **1a** at room temperature was studied previously by Lockhart [8], but he reported only one broadened methyl resonance for **1a**, ascribing the considerable linewidth to low crystallinity in the sample. In particular, the possibility of molecular motion as the possible cause for the linebroadening was not discussed. Finally, we note that no such temperature-dependent effects were observed for $(^iBu_3Sn)_2CO_3$, **1b**.

Acknowledgements

Support of our work by the Deutsche Forschungsgemeinschaft is gratefully acknowledged.

References

1 P. Kulmitz, J. Prak. Chem., 80 (1860) 60.
2 H. Sato, and R. Okawara, Proc. Int. Symp. Mol. Struct. Spectroscopy, Tokyo (1962) A308.
3 D.H. Lohmann, J. Organomet. Chem., 4 (1965) 382.

4 B.Y.K. Ho and J.J. Zuckerman, J. Organomet. Chem., 96 (1975) 41.
5 A.G. Davies and P.J. Smith, in G. Wilkinson, F.G.A. Stone and E.W. Abel (Eds.), Comprehensive Organometallic Chemistry, Vol. 2, Pergamon Press, Oxford 1982.
6 S.J. Blunden, R. Hill and J.N.R. Ruddick, J. Organomet. Chem., 267 (1984) C5.
7 E.R.T. Tiekink, J. Organomet. Chem., 302 (1986) C1.
8 T.P. Lockhart and W.F. Manders, J. Am. Chem. Soc., 107 (1985) 5683.
9 T.P. Lockhart, J. Organomet. Chem., 287 (1985) 179.
10 R.K. Harris and A. Sebald, Magn. Reson. Chem., 25 (1987) 1058.
11 B.Y.K. Ho and J.J. Zuckerman, Inorg. Chem., 12 (1973) 1552.
12 J.G.A. Luijten, Recl. Trav. Chim. Pays-Bas, 82 (1963) 1179.
13 H. Kriegsmann, H. Hoffmann and S. Pischtschan, Z. Anorg. Allg. Chem., 315 (1962) 283.
14 C.A. Kraus and R.H. Bullard, J. Am. Chem. Soc., 51 (1929) 3605.
15 W.P. Neumann and G. Burckhardt, Ann., 663 (1963) 11.
16 G. Güttner and E. Krause, Chem. Ber., 50 (1917) 1802.
17 W.P. Neumann, B. Schneider and R. Sommer, Ann., 692 (1966) 1.
18 International Tables for X-Ray Crystallography, Vol. 1, Kynoch Press, Birmingham, 1974.
19 G.M. Sheldrick, SHELXS 86, Program for crystal structure determination, Göttingen 1986.
20 G.M. Sheldrick, SHELX 76, Program for crystal structure determination, Cambridge 1976.
21 R. Hundt, KPLOT, A Program for Drawing and Studying Crystal Structures, Bonn 1979.
22 C.K. Johnson, ORTEP, A Fortran Thermal Ellipsoid Plot Program for Crystal Structure Illustrations, Oak Ridge 1965; modified by R. Hundt, Bonn, 1969.
23 H. Reuter and H. Puff, J. Organomet. Chem., 379 (1989) 223.
24 C. Glidewell and D.C. Liles, Acta Crystallogr., B34 (1978) 1693.
25 C. Glidewell and D.C. Liles, Acta Crystallogr., B35 (1979) 1689.
26 S. Kerschl, D. Wrackmeyer, D. Männig, H. Nöth and R. Staudigl, Z. Naturforsch., B42 (1987) 387.
27 H. Reuter, PhD Thesis, Bonn, 1987.
28 T.P. Lockhart, H. Puff, W. Schuh, H. Reuter and T.N. Mitchell, J. Organomet. Chem. 366 (1989) 61.
29 U. Weber, N. Pauls, W. Winter and H.B. Stegmann, Naturforsch., B37 (1982) 1316.
30 S. Masamume, L.R. Sita and D.J. Williams, J. Am. Chem. Soc., 105 (1983) 630.
31 H. Puff, W. Schuh, R. Sievers, W. Wald, and R. Zimmer, J. Organomet. Chem., 240 (1984) 271.
32 W. Wald, PhD Thesis, Bonn, 1987.
33 C. Glidewell and D.C. Liles, Acta Crystallogr., B34 (1978) 124.
34 D. Tudela, private communication.
35 U. Grummisch, PhD Thesis, Bonn, 1987.
36 J.F. Vollano, R.O. Day and R.R. Holmes, Organometallics, 3 (1984) 745.
37 H. Puff, E. Friedrichs and F. Visel, Z. Anorg. Allg. Chem., 477 (1981) 50.
38 R.K. Harris and A. Sebald, Magn. Reson. Chem., 27 (1989) 81.
39 R.K. Harris, A. Sebald, D. Furlani, and Tagliavini, G. Organometallics, 7 (1988) 388.
40 R.K. Harris and A. Sebald, J. Organomet. Chem., 331 (1987) C9.
41 K.C. Molloy, Inorg. Chim. Acta, 141 (1988) 151.
42 P.A. Bates, M.B. Hursthouse, A.G. Davies and S.D. Slater, J. Organomet. Chem., 363 (1989) 45.
43 R.K. Harris, K.J. Packer, P. Reams, and A. Sebald, J. Magn. Reson., 72 (1987) 385.
44 M. Mehring, Principles of High Resolution NMR in Solids, Springer-Verlag, Berlin, 1983.
45 P.S. Allen and A. Cowking, J. Chem. Phys., 47 (1967) 4286.
46 J. Kümmerlen and A. Sebald, J. Am. Chem. Soc., in preparation.
47 K.L. Walther A. Wokaun and A. Baiker, Mol. Phys., 71 (1990) 769.